Doxorubicin Loaded-UiO-66-NH2 Coated With Poly(N-Vinylcaprolactam) For Controlled Release of Doxorubicin Against A549 Lung Cancer

Navid Rakhshani
Islamic Azad University
nahid Hassanzadeh Nemati (nahid_hasanzadeh@yahoo.com)
Islamic Azad University Science and Research Branch https://orcid.org/0000-0003-1725-8430
Ahmad Ramazani Saadatabadi
Sharif University of Technology
S.K. Sadrnezhaad
Sharif University of Technology

Research Article

Keywords: Metal-organic framework, UiO-66-NH2, Poly(N-Vinylcaprolactam), Doxorubicin, Lung cancer

Posted Date: May 5th, 2021

DOI: https://doi.org/10.21203/rs.3.rs-483360/v1

Abstract

The use of nano metal-organic frameworks (NMOFs) has been developed for drug delivery systems due to their high porosity and large specific surface area. In this work, UiO-66-NH_2 NMOFs were synthesized via the microwave heating method and doxorubicin (DOX) molecules were incorporated into the UiO-66-NH_2 NMOFs. Then, poly(N-Vinylcaprolactam) (PNVCL) synthesized by the free radical polymerization was coated on the NMOFs surface to fabricate the pH/temperature-sensitive carrier against A549 lung cancer cells death in vitro. The synthesized nanocarriers were characterized using FTIR, XRD, SEM, FESEM, TGA, and BET analysis. The average particle sizes of UiO-66-NH_2 MOF and PNVCL coated-UiO-66-NH_2 /DOX MOF nanoparticles were found to be 175 nm and 235 nm, respectively. TGA analysis showed that the PNVCL percentage coated on the UiO-66-NH_2 NMOFs surface was about 17.5 %, and 27.3% for NMOFs incubated in 1% and 2% PNVCL solutions, respectively. The BET surface area of UiO-66-NH_2 NMOFs, UiO-66-NH_2 NMOFs/DOX 100 µg mL^{-1}, and PNVCL 1% coated-NMOFs/DOX was found to be 1052, 121, and 87 m^2g^{-1}, respectively. The DOX release data of UiO-66-NH_2 and PNVCL coated- UiO-66-NH_2/DOX were evaluated under pH values of 5.5, 7.4, and temperatures of 25 °C, 37°C. The anticancer activity of synthesized NMOFs was investigated against lung cancer cells (A549) in vitro. The maximum cytotoxicity of A549 cancer cells was found to be 76% using PNVCL 1% coated-UiO-66-NH_2/DOX 100 µg mL^{-1} NMOFs.

1. Introduction

Metal-organic frameworks (MOFs) as crystalline porous materials have been widely used for targeted delivery of anticancer drugs due to their high specific surface area, large porosity, good biocompatibility, and fine pore sizes [1-7]. The nanosized-MOFs (NMOFs) prepared by the microwave heating method exhibited unique physic-chemical properties in comparison to the micrometer scale of MOFs [1, 8]. The advantages of MOFs compared with other inorganic drug delivery systems (DDS) are the high encapsulation efficiency and their easier functionalization for targeted delivery [9-14]. UiO-66 MOFs ([Zr6O4(OH)4]) with high stability and high biocompatibility as well as good biodegradability and high specific surface area had a high potential for delivery of anticancer drugs [15-17]. Furthermore, UiO-66 MOFs with Zr-O clusters, and metal sites, as well as octahedral and tetrahedral cavities, could be considered for the controlled release of Doxorubicin (DOX) due to having a coordination interaction between the Zr (IV) clusters of UiO-66 and hydroxyl groups of DOX [4, 18]. Moreover, the presence of open cavities and clusters in the UiO-66 MOFs matrix causes the incorporation of the high content of drug molecules, and following its release could occur in a controlled manner. UiO-66 MOF is also a good candidate for the controlled release of anticancer agents into the cancer tissues as a pH-sensitive carrier [18]. Thus, DOX could be released from UiO-66 MOFs into the acidic tumor sites due to the protonation of phosphate and weaknesses of the interaction between DOX and Zr-O clusters of UiO-66 MOF under acidic condition [18, 19].

The accumulation of NMOFs in the bloodstream could be decreased by the coating of NMOFs surface with polymers which improve the stability of NMOFs and provide the effective application of NMOFs in DDSs of anticancer drugs during the in vitro and in vivo therapy of various cancers through the targeted delivery of anticancer agents into the tumor tissues [20-22]. Furthermore, the specific distribution of anticancer drugs on the cancerous cells could decrease the adverse side effects of anticancer drugs via decreasing the non-selective distribution of drugs on the healthy cells. The coating of stimuli-responsive polymers on the MOFs surface could result in the enhancement of the permeability of the anticancer drug on the cancerous cells [23-26].

The lower critical solubility temperature (LCST) thermoresponsive polymers such as poly (N-isopropyl acrylamide) (PNIPAAm), and poly (N-vinyl caprolactam) (PNVCL) have been developed for DDSs of anticancer drugs [27-30]. Among LCST polymers, PNVCL as a hydrophilic biocompatible temperature-sensitive polymer is used for various biomedical applications [30-34]. Furthermore, the biocompatibility of PNVCL is higher than PNIPAAm, due to the hydrolysis of acrylamide groups of PNIPAAm and the production of small compounds which is not suitable for biomedical applications [35]. The LCST of PNVCL is ranging from ~32-34° which is close to physiological temperature. Thus the release rate could be controlled by the coating of PNVCL on the MOF surface at body temperature through the delay in the release of anticancer agents.

In the present study, UiO-66-NH_2 NMOFs were synthesized via the microwave heating method and DOX molecules were loaded into the NMOFs. Then, its surface was coated with PNVCL. The synthesized NMOF and PNVCL coated-nanoparticles were characterized using FTIR, XRD, SEM, FESEM, TGA, and BET analysis. The release profiles of DOX from UiO-66-NH_2 and PNVCL coated UiO-66/DOX were studied under different pH values and temperatures. The anticancer activity of synthesized NMOFs was investigated against A549 lung cancer cells in vitro.

2. Experimental

2.1 Materials

2-amino terephthalic acid (BDC-NH2, purity ≥ 99.9%), zirconium chloride (ZrCl4, purity ≥ 99.9%) supplied from Sigma–Aldrich (Germany) and N, N Dimethylformamide (DMF, purity≥99.0%), hydrochloric acid (HCl, 37%) purchased from Fluka (Switzerland) were used for the synthesis of UiO-66-NH_2 MOF nanoparticles. N-Vinylcaprolactam (NVCL), 2,20-Azoisobutyronitrile (AIBN), 3-mercaptopro-pionic acid (MPA), and diethyl ether provided from Sigma-Aldrich (Germany) were used for the synthesis of PNVCL.

2.2 Synthesis of UiO-66-NH_2 and UiO-66-NH_2/DOX

UiO-66-NH_2 NMOFs were synthesized via the microwave method as described in reference [5]. Briefly, $ZrCl_4$ (125mg) and BDC-NH_2 (134mg) were dispersed into the 15 mL DMF and 1 mL HCl under sonication

for 1 h. Then, the mixture was transferred into the microwave and the heating proceeded at 130°C for 1h. Then, the product was washed with DMF and methanol three times and was dried at 60 °C for 6 h.

To load DOX molecules into the UiO-66-NH_2 MOF, 5 mg of UiO-66-NH_2 NMOFs were dispersed into DOX solutions (10, 50, and 100 μg mL^{-1}) for 24 h under stirring. Then, the prepared UiO-66-NH_2/DOX was washed with ethanol and distilled water three times. Then, the prepared products were centrifuged at 12000 rpm for 20 min. The final content of DOX in NMOFs samples was determined according to the initial content of DOX, the final content of DOX in solution, and DOX content in the supernatant after centrifugation of NMOFs using UV-Vis spectrophotometer at a wavelength of 481 nm. The drug encapsulation DEE (%) is evaluated as follows:

$$DEE\,(\%) = \frac{Final\ \ content\ \ of\ \ drugs\ \ in\ \ samples}{Initial\ \ content\ \ of\ \ drugs\ \ in\ \ solution} \times 100\,\% \quad \text{(Eq. 1)}$$

2.3 Synthesis of PNVCL and PNVCL coated- UiO-66-NH_2/DOX

The carboxylated PNVCL is synthesized by free radical polymerization of NVCL, MPA, and AIBN in isopropanol at 70 °C for 8 h. Then, diethyl ether was added to precipitate the synthesized product. Later, the precipitated product was dried under vacuum. The prepared sample was dispersed in deionized water and was dialyzed for 4 days (MWCO of 5000) to remove the unreacted materials. Finally, the obtained product was lyophilized.

To coat the UiO-66-NH_2/DOX surface with PNVCL, the predetermined amount of MOF nanoparticles was dispersed in 1% and 2% PNVCL (dissolved in distilled water) under stirring for 24 h and then, centrifuged at 12000 rpm for 39 min to remove the non-attached PNVCL on the MOFs surface. The prepared UiO-66-NH_2/DOX/PNVCL samples were washed three times with deionized water and dialyzed for 3 days (MWCO of 12000) and then dried at 30°C for 24 h. Finally, the obtained product was lyophilized for further investigations. The schematic of the PNVCL and PNVCL/UiO-66-NH_2/DOX synthesis is illustrated in Fig.1.

2.4 Characterization tests

The X-ray diffraction (XRD) patterns were recorded using Philips X'pert diffractometer in the range of 10–80° at 2θ with Cu-Kα radiation. To analyze the functional groups of UiO-66-NH_2, UiO-66-NH_2/DOX, PNVCL, and UiO-66/DOX/PNVCL, the FTIR spectra of samples were conducted on an Equinox 55 FTIR spectrometer in the range of 4000-400 cm^{-1}. The hydrodynamic diameter and size distribution of the UiO-66 MOFs and DOX loaded-MOFs were determined using dynamic light scattering (DLS) by a Malvern Zetasizer Nano (Malvern Instruments, Worcestershire). The scanning electron microscopy (SEM, JEOL JSM-6380) and field emission scanning electron microscopy (FESEM, MIRA3TESCAN-XMU) were applied to compare the morphology and structure of UiO-66-NH_2/DOX and PNVCL coated- UiO-66-NH_2/DOX MOF

nanoparticles. The thermal analysis of UiO-66-NH_2/DOX and PNVCL coated- UiO-66-NH_2/DOX MOF nanoparticles was carried out using thermogravimetric analysis (TGA Q500) by the heating rate of 10 °C min^{-1} ranging from 50-700°C. The Brunauer-Emmett- Teller (BET) method was used to measure the specific BET surface area of MOFs (Micromeritics ASAP 2010, Micromeritics, Norcross, GA, USA) by the N2 adsorption-desorption isotherm. The UV-Vis spectrophotometer (JAS.CO V-530, Japan) was used to measure the final concentration of DOX at a wavelength of 481 nm.

2.5 Drug release and kinetic studies

To obtain the DOX release behavior from synthesized MOFs, the drug loaded-MOFs were incubated in 50 mL of 0.1 M phosphate buffer solution at temperatures of 25, 37 °C and pH values of 5.5, 7.4. At predetermined time intervals, 2 mL of incubation solution was collected from the solution medium. While 2 mL of fresh PBS was simultaneously added into the dissolution medium. The DOX release was determined according to its concentration at a certain time and actual drug content in MOFs. The release experiments were carried out three times and the average values were reported. The kinetic data of DOX release were analyzed by the zero-order, Higuchi [36], and Korsmeyer-Peppas [37] pharmacokinetic models to obtain the drug release mechanism from synthesized MOFs.

2.6 Cell viability

To investigate the biocompatibility of MOFs samples, the synthesized nanoparticles were incubated in the L929 normal fibroblast cells (Institute Pasteur of Iran, IPI, Tehran, Iran) cultured in RPMI with 10% fetal calf serum and 1% penicillin-streptomycin at 37°C in a humidified atmosphere of 5% CO2. The cell viability of synthesized DOX loaded-MOF nanoparticles (100 µg/mL) against A549 lung cancer cell lines (IPI, Tehran, Iran) was evaluated after 24, 48, and 72 h incubation time as described previously [38]. The ELISA microplate reader (Multiskan MK3, Thermo Electron Corporation, USA) at a wavelength of 570 nm was used to determine the cell viability of A549 cells treated with MOF nanoparticles. The CyFlow flow cytometer (Partec, Germany) by staining of cells with Annexin V-fluorescein isothiocyanate (VFITC) /propidium iodide (PI) was used to compare the apoptosis of A549 cancer cells in the presence of various MOFs samples [39].

3. Results

3.1 Characterization of MOF nanoparticles

The XRD patterns of UiO-66-NH_2 MOF and PNVCL coated UiO-66-NH_2/DOX MOF nanoparticles are illustrated in Fig.2. The presence of sharp diffraction peaks at 2θ=7.5˚ and 8.5˚ corresponding to (111), and (002) planes indicated the formation of pure UiO-66-NH_2 MOF nanoparticles [5]. The SEM images and FESEM images of UiO-66-NH_2 MOF and PNVCL coated- UiO-66-NH_2/DOX MOF nanoparticles are illustrated in Fig.3. As shown, the uniform nanoparticles ranging from 100-200 nm were obtained for UiO-66-NH_2 MOF particles. The FESEM image of synthesized UiO-66-NH_2 MOF nanoparticles revealed the

presence of irregular shapes (spherical and polyhedral) of UiO-66-NH_2 MOF nanoparticles with an average particle size of 175 nm. The SEM image of PNVCL coated-UiO-66-NH_2/DOX MOF indicated the increase in the particle sizes of particles. The particle sizes were obtained ranging from 100-300 nm with an average particle size of 235 nm. The increase in particle sizes was further confirmed by the dynamic light scattering (DLS) measurements. As shown, the average hydrodynamic sizes of UiO-66-NH_2 NMOFs and DOX loaded-UiO-66-NH_2 NMOFs were about 230 nm and 275 nm, respectively.

Fig.2 XRD patterns of UiO-66-NH_2 MOF and PNVCL coated- UiO-66/DOX MOF nanoparticles

Fig.3 (a) SEM and (b) FESEM images of UiO-66-NH_2 MOF (c) SEM and (d) FESEM images PNVCL 1% coated- UiO-66-NH_2/DOX MOF nanoparticles and (e) DLS of UiO-66-NH_2 NMOFs and DOX loaded-UiO-66-NH_2 NMOFs

The FTIR spectra of UiO-66-NH_2, UiO-66-NH_2/DOX, PNVCL, and UiO-66-NH_2/DOX/PNVCL are illustrated in Fig.4. For UiO66-NH_2 MOF nanoparticles, the observed peaks at 3450 cm^{-1} and 3360 cm^{-1} were attributed to the OH and NH stretching vibrations, respectively. The carboxylate groups of BDC-NH_2 in the UiO-66-NH_2 structure were detected at 1575 $cm^{-1}$and 1390 cm^{-1}. The observed peaks at 730 cm^{-1}, 665 cm^{-1}, and 560 cm^{-1}were attributed to the Zr(μ_3) O bands of MOF. The amide stretching vibration was detected at around 1730 cm^{-1} for pure UiO-66-NH_2 MOF nanoparticles. The observed new peaks at 1710 cm^{-1} and 1610 cm^{-1} corresponding to the C=O and C=C groups of DOX, demonstrated the loading of DOX molecules into the UiO66-NH2 NMOFs. Furthermore, the peaks of carboxylate groups of NMOFs were shifted from 1575 cm^{-1} and 1390 cm^{-1} to 1588 cm^{-1} and 1410 cm^{-1} after loading of DOX molecules into the NMOFs. For carboxylated PNVCL, the appeared bonds at 3425 cm^{-1}, 2920 cm^{-1}, 1620 cm^{-1}, 1480 cm^{-1}, 1420 cm^{-1}, and 840 cm^{-1} were attributed to the carboxylic groups, –CH aliphatic groups, amide I absorption band, C-N and C-H stretching vibrations. For PNVCL coated NMOFs, the carbonyl peak intensity was increased at around 1720 cm^{-1}.

The thermogravimetric analysis of UiO-66-NH_2 NMOFs and PNVCL (1% and 2%) coated- UiO-66-NH_2 NMOFs are illustrated in Fig.5. For UiO-66-NH_2 NMOFs, three steps of weight loss occurred. The weight loss at temperatures lower than 200 °C could be attributed to the evaporation of solvents. The second weight loss ranging from 200-300 °C was due to the dihydroxylation of $Zr_6O_4(OH)_4$ to Zr_6O_6 [43]. The main weight loss after 400 °C could be attributed to the decomposition of organic groups. For PNVCL coated-UiO-66-NH_2 NMOFs, the weight loss after 350 °C was attributed to the pyrolysis of the PNVCL chains and decomposition of organic linkers of UiO-66-NH_2.

The adsorption/desorption isotherms for UiO-66-NH_2, UiO-66-NH_2/DOX and PNVCL coated- UiO-66-NH_2/DOX are illustrated in Fig.6. For UiO-66-NH_2, the BET surface area and pore volume were found to be 1052 m^2g^{-1}, and 0.58 cm^2g^{-1}, respectively. After loading DOX into the NMOFs, the BET surface area and pore volume were decreased to 121 m^2g^{-1} and 0.12 cm^2g^{-1}, respectively which demonstrated the high

loading of DOX molecules into the pores of nanofibers. The blockage of NMOFs pores with DOX molecules resulted in a significant decrease in specific BET surface area after loading of DOX into the NMOFs. After the coating of PNVCL, the specific BET surface area and pore volume were decreased to 87 m^2g^{-1} and 0.08 cm^2g^{-1}, respectively.

3.2 Drug encapsulation efficiency, drug release, and kinetic studies

The DOX encapsulation efficiency for NMOFs incubated at 10, 50 and 100 μgmL^{-1} DOX is presented in Table 1. As shown in this table, the maximum drug encapsulation efficiency (DEE%) was found to be 55.5% from 1% PNVCL coated-NMOFs containing 10 µg/mL DOX. By increasing DOX concentration, the DEE was gradually decreased. Furthermore, a coating of 2% PNVCL on the NMOFs surface resulted in a decrease of DEE in comparison to DEE of PNVCL 1% coated-NMOFs in the same condition.

Table 1 Drug loading efficiency of synthesized UiO-66-NH_2/DOX/PNVCL NMOFs (n=5)

PNVCL concentration (%)	DOX concentration (μgm^{-1})	Drug loading efficiency (%)
1	10	55.5±2.3
1	50	52.6±2.1
1	100	49.9±1.6
2	10	46.6±1.5
2	50	42.2±1.4
2	100	38.9±1.3

The DOX release profiles of NMOFs containing 50 µg mL^{-1} DOX at temperatures of 25 °C, 37 °C and pH values of 5.5 and 7.4 are illustrated in Fig. 7. As can be seen, the increase in pH from 5.5 to 7.4 and temperature from 25 °C to 37 °C resulted in a slower release of DOX from NMOFs coating with 1% and 2% PNVCL. Thus, the fastest release was achieved at pH of 5.5 and temperature of 25 °C. About 80% DOX release occurred from 1% PNVCL coated NMOFs after 48 h, 60 h, 72 h, and 120 h at pH of 5.5, temperature of 25 °C, pH of 7.4, Temperature of 25 °C, pH of 5.5, Temperature of 37 °C and pH of 7.4, Temperature of 37 °C. Although, the DOX release mechanism was dependent on the temperature and pH variations, the effect of temperature on the release rate of DOX and its slower release was higher than that of pH effect on the declining release rate of DOX from NMOFs.

The comparison of correlation coefficients of pharmacokinetic models indicated that the Korsmeyer-Peppas model ($R^2 > 0.99$) was best described the DOX release data (Table 2). Furthermore, the "n" values

of the Korsmeyer-Peppas equation indicated the non-Fickian diffusion of the DOX release data of NMOFs under pH of 5.5, Temperature of 25 °C, pH of 7.4, Temperature of 25 °C and pH of 5.5, Temperature of 37 °C and Fickian diffusion of the DOX release data of NMOFs at pH of 7.4 and Temperature of 37 °C.

Table 2 Pharmacokinetic parameters of DOX release from NMOFs

Nanocarrier	pH	Temperature (°C)	Zero-order		Higuchi		Korsmeyer-Peppas		
			K_0 (hr^{-1})	R^2	K_H ($hr^{-0.5}$)	R^2	n	K_{KP}	R^2
UiO-66/DOX/PNVCL 1%	7.4	25	0.222	0.932	2.952	0.944	0.664	3.65	0.995
	7.4	37	0.182	0.944	2.545	0.955	0.410	2.98	0.994
	5.5	25	0.232	0.925	3.192	0.954	0.712	4.23	0.993
	5.5	37	0.202	0.936	2.777	0.950	0.548	3.33	0.994
UiO-66/DOX/PNVCL 2%	7.4	25	0.218	0.935	2.811	0.954	0.601	3.44	0.994
	7.4	37	0.175	0.939	2.324	0.960	0.384	2.62	0.993
	5.5	25	0.212	0.932	2.944	0.950	0.652	3.86	0.996
	5.5	37	0.196	0.943	2.553	0.958	0.508	3.11	0.995

3.3 Cytotoxicity of NMOFs

The cytotoxicity of UiO-66-NH_2, UiO-66-NH_2/PNVCL 1%, and UiO-66-NH_2/PNVCL 2% against normal fibroblast cells are illustrated in Fig. 8a. The gradual decrease in the cell viability of pure UiO-66-NH2 by time could be attributed to the Zr-O clusters release into the medium which increased the cytotoxicity of cells treated with fibroblast cells treated with UiO-66-NH_2 NMOFs. Whereas, there was no significant cytotoxicity toward fibroblast normal cells treated with PNVCL coated-NMOFs.

The cytotoxicity of pure UiO-66-NH_2 NMOFs, pristine DOX (100 µg mL^{-1}), UiO-66-NH_2/DOX 50 µg mL^{-1}, UiO-66-NH_2/DOX 100 µg mL^{-1}, PNVCL 1% and PNVCL 2% coated- UiO-66-NH_2/DOX NMOF samples against A549 lung cancer cells is illustrated in Fig.8b. As shown, there was a little cytotoxicity of UiO-66-NH_2NMOFs against A549 cells after 72 h. The cytotoxicity of pure DOX was found to be 66% against A549 lung cancer cells. By loading 50 and 100 µg mL^{-1} DOX into the UiO-66-NH_2NMOFs, the cytotoxicity of NMOFs was increased to 56% and 45% against A549 lung cancer cells after 72 h incubation time for the UiO-66-NH_2/DOX 50 µg $mL^{-1}$and UiO-66-NH_2/DOX 100 µg mL^{-1}, respectively. The maximum

cytotoxicity of A549 cancer cells was about 76% in the presence of PNVCL 1% coated- UiO-66-NH_2/DOX 100 µg mL^{-1} NMOFs. Coating of NMOFs with 2% PNVCL resulted in decreasing the cytotoxicity of NMOFs against A549 cancer cells.

The DAPI staining images of untreated A549 cells and A549 cells treated UiO-66-NH_2/DOX 100 µg mL^{-1} NMOFs and NMOFs coated with 1% and 2% PNVCL after 72 h incubation time are illustrated in Fig. 9. As shown, the nuclear fragmentation in their chromatin of cells was detected in the presence of 100 µg mL^{-1} DOX loaded- NMOFs and NMOFs/DOX coated with 1% and 2% PNVCL.

4. Discussion

The comparison of XRD patterns of UiO-66-NH_2 MOF and PNVCL coated UiO-66-NH_2/DOX MOF indicated that the incorporation of DOX into the MOF and coating with PNVCL resulted in the weakening of diffraction peaks of UiO-66-NH_2 MOF due to decreasing the X-ray contrast of MOF pore cages. Furthermore, no diffraction peaks were detected in the XRD pattern of PNVCL coated-UiO-66-NH_2/DOX MOF nanoparticles which indicated the amorphous status of PNVCL and DOX in the UiO-66/DOX/PNVCL matrix. The increase in the particle size of UiO-66/DOX/PNVCL was due to the incorporation of DOX molecules into the MOF nanoparticles and its coating with PNVCL polymer. The FESEM image of PNVCL 1% coated- UiO-66-NH_2/DOX particles demonstrated an appropriate coating of the UiO-66-NH_2 surface with PNVCL. The comparison of SEM and DLS results indicated that the average particle sizes of synthesized NMOFs reported by SEM were lower than that of DLS. The hydrodynamic radius of MOFs was found to be higher than that of particle sizes of dried nanoparticles. Similar trends were reported by other researchers [40, 41]. The comparison of FTIR spectra of pure PNVCL and PNVCL 1% coated- UiO-66-NH_2/DOX indicated that the carboxyl peak intensity in the FTIR spectrum of UiO-66-NH_2/DOX/PNVCL was decreased in comparison to the carboxyl peak intensity of pure PNVCL which could be attributed to the interaction of carboxylic groups of PNVCL with amine groups of UiO-66-NH_2 [42]. Furthermore, the appeared new band at 1522 cm-1 corresponding to the amide II groups revealed the interaction of PNVCL polymer and UiO-66-NH_2 NMOFs. The comparison of TGA curves of UiO-66-NH_2 NMOFs, and PNVCL (1% and 2%) coated- UiO-66-NH_2 NMOFs indicated that the polymer percentages coated on the UiO-66-NH_2 NMOFs surface were found to be 17.5 %, and 27.3% for NMOFs incubated in 1% and 2% PNVCL solution, respectively. The BET analysis results indicated that the blockage of NMOFs pores with DOX molecules resulted in a significant decrease in specific BET surface area after loading of DOX into the NMOFs. After the coating of PNVCL, the specific BET surface area and pore volume were decreased to 87 m^2g^{-1} and 0.08 cm^2g^{-1}, respectively in comparison to high BET surface area (1052 m^2g^{-1}) and high pore volume of bare UiO-66-NH_2 NMOFs (0.58 cm^2g^{-1}).

The release profiles results indicated the faster release of DOX from PNVCL 1% coated-NMOFs in comparison to PNVCL 2% coated-NMOFs. This behavior could be attributed to the easier diffusion of DOX

molecules from NMOFs containing PNVCL 1% due to the lower thickness of PNVCL formed on the NMOFs surface. The loss of some interactions between Zr-O clusters/DOX and UiO-66-NH_2/PNVCL resulted in the faster release of DOX from NMOFs at pH of 5.5 in comparison to DOX release at pH of 7.4. At 25 °C, the swelling of PNVCL ON THE NMOFs surface resulted in a faster release of DOX from NMOFs. Whereas, the collapse of the PNVCL matrix at temperature higher than LCST (lower critical solution temperature) of PNVCL (32 °C) resulted in slower diffusion of drug molecules from PNVCL and slower release of DOX at physiological temperature. A similar trend was reported by Rao et al. for 5-FU release from PNVCL nano gel [31].

The biocompatibility of UiO-66-NH_2/PNVCL 1% and UiO-66-NH_2/PNVCL 2% was higher than pure UiO-66-NH_2 NMOFs due to its coating with biocompatible PNVCL. The gradual cytotoxicity of UiO-66-NH_2NMOFs against A549 cells after 72 h was due to the release of clusters of UiO-66-NH_2 NMOFs into the medium. The controlled release of DOX from DOX loaded- UiO-66-NH_2NMOFs is responsible for higher antitumor efficacy of DOX loaded-UiO-66-NH_2NMOFs in comparison to pristine DOX. The coating of PNVCL on the UiO-66-NH_2/DOX surface resulted in the continuous release of DOX and enhancement in cytotoxicity after 72 h. Whereas, the lower cytotoxicity of PNVCL 1% and 2% coated- UiO-66-NH_2/DOX after 24 h incubation time in comparison to the cytotoxicity of UiO-66-NH_2/DOX could be attributed to the lower content of DOX in the medium due to the sustained release of DOX from PNVCL coated UiO-66-NH_2/DOX. The DAPI staining results indicated the higher fragmentized nuclei of cells treated with UiO-66-NH_2/DOX 100 μg mL^{-1}/PNVCL 1%. Therefore, this formulation could be considered as an optimum formulation for the A549 cancer cells death.

5. Conclusion

The PNVCL coated- UiO-66-NH_2/DOX NMOFs were successfully synthesized and its application was investigated for controlled release of DOX against A549 lung cancer cells. The XRD and FESEM image of UiO-66-NH_2 NMOFs demonstrated the formation of crystalline nanoparticles with an average particle size of 175 nm. The FTIR spectra of PNVCL coated NMOFs revealed the interaction of carboxylic groups of PNVCL with amine groups of UiO-66-NH2. Based on TGA results, the PNVCL polymer percentages coated on the UiO-66-NH_2 NMOFs surface were found to be 17.5 %, and 27.3% for NMOFs incubated in 1% and 2% PNVCL solutions. The BET surface area and pore volume of UiO-66-NH_2 NMOFs were found to be 1052 m^2g^{-1}, and 0.58 cm^2g^{-1}, respectively. The maximum drug encapsulation efficiency (DEE %) was found to be 55.5% from NMOFs coated with 1% PNVCL and 10 μg mL^{-1} DOX. The DOX release percentage from 1% PNVCL coated NMOFs was achieved to 80% within 48 h, 60 h, 72 h, and 120 h under pH of 5.5, temperature of 25 °C, pH of 7.4, the temperature of 25 °C, pH of 5.5, the temperature of 37 °C and pH of 7.4, the temperature of 37 °C. The Korsmeyer-Peppas model was best described the DOX release data of synthesized NMOFs. There was no significant cytotoxicity toward fibroblast normal cells treated with PNVCL coated-NMOFs. Whereas, the maximum cytotoxicity of A549 cancer cells was about 76% in the presence of PNVCL 1% coated- UiO-66-NH_2/DOX 100 μg mL^{-1} NMOFs. Therefore, the loading of DOX into

the NMOFs, and its surface coating with PNVCL improved the efficiency of chemotherapy for targeted delivery of DOX against lung cancer compared to unloaded DOX.

References

1. A.R. Abbasi, S. Hatami, J. Inorg. Organomet. Polym Mater. **27**, 1941 (2017)
2. S. Beg, M. Rahman, A. Jain, S. Saini, P. Midoux, C. Pichon, F.J. Ahmad, S.Akhter. Drug Discov. Today **22**, 625 (2017)
3. D. Wei, Y. Xin, Y. Rong, Y. Li, C. Zhang, Q. Chen, S. Qin, W. Wang, Y. Hao.. J Inorg Organomet Polym Mater **30**, 1121 (2020)
4. A. Bhattacharjee, M.K. Purkait, S. Gumma, J. Inorg. Organomet. Polym Mater. **30**, 2366 (2020)
5. A. Bazzazzadeh, B.F. Dizaji, N. Kianinejad, A. Nouri, M. Irani. Int. J. Pharm. **587**, 119674 (2020)
6. J.R. Bi, Y. Zheng, L.Q. Fang, Y.C. Guan, A.Q. Ma, J. Wu. J Inorg Organomet Polym Mater **30**, 3388 (2020)
7. A. Farboudi, K. Mahboobnia, F. Chogan, M.Karimi,A. Askari, S. Banihashem, S. Davaran, M.Irani. Int. J. Biol. Macromol. **150**, 178 (2020)
8. P. Kush, T. Bajaj, M. Kaur, J. Madan, U.K. Jain, P. Kumar, A. Deep, K.H. Kim, J. Inorg. Organomet. Polym Mater. **30**, 2827 (2020)
9. F.Su,Q. Jia, Z. Li, M. Wang, L. He, D. Peng, Y. Song, Z. Zhang, S.Fang. Microporous Mesoporous Mater. **275**, 152 (2019)
10. A.R. Chowdhuri, T. Singh, S.K. Ghosh, S.K. Sahu, ACS Appl **8**, 16573 (2016)
11. B.M. Jarai., Z. Stillman, L. Attia, G.E. Decker, E.D. Bloch, C.A. Fromen, ACS Appl **12**, 35 (2020)
12. M.X. Wu, Y.W. Yang, Adv. Mater **29**, 1606134 (2017)
13. X. Ke, N. Qin, T. Zhang, F. Ke, X. Yan, J. Inorg. Organomet. Polym Mater. **30**, 935 (2020)
14. A. Ebrahimpour, N.R. Alam, P. Abdolmaleki, B. Hajipour-Verdom, F. Tirgar, T. Ebrahimi, M. Khoobi, J. Inorg. Organomet. Polym Mater. **31**, 1208 (2021)
15. J. X.Zhu.Gu, Y.Wang, B.Li, Y.Li, W..Zhao, J.Shi. ChemComm **50**, 8779 (2014)
16. I.A. Lázaro, S. Haddad, S. Sacca, C.Orellana -Tavra, D.F. Jimenez, R.S. Forgan. Chem **2**, 561 (2017)
17. M. Nasrabadi, M.A. Ghasemzadeh, M.R. Zand Monfared. New J Chem **43**, 16033 (2019)
18. A.R. Chowdhuri, D. Laha, S. Chandra, P. Karmakar, S.K..Sahu. Chem. Eng. J. **319**, 200 (2017)
19. H.X. Zhao, Q. Zou, S.K. Sun, C.Yu,X. Zhang, R.J. Li, Y.Y.Fu. Chem. Sci. **7**, 5294 (2016)
20. J. L.Tang.Shi, X.Wang, S..H. Zhang.H. Wu.Sun, Z.Jiang. Nanotechnology **28**, 275601 (2017)
21. C.S. Y.Liu, Gong, Y.Dai, Z.Yang, G..Y. Yu.Liu, M.Zhang,. Biomaterials **218**, 119365 (2019)
22. A. D.Giliopoulos.D. Zamboulis.D. Giannakoudakis.Bikiaris, K.Triantafyllidis. Molecules **25**, 185 (2020)
23. W.Cai,J. Wang, C. Chu, W. Chen, C. Wu, G.Liu. Adv. Sci. **6**, 1801526 (2019)
24. C. Liu, X. Xu, J. Zhou, J.Yan,D. Wang, H.Zhang. BMC Mater **2**, 1 (2002)

25. S. Javanbakht, M. Pooresmaeil, H.Hashemi, HNamazi. Int. J. Biol. Macromol. **119**, 588 (2018)
26. T.A. Vahed, M.R. Naimi-Jamal, L.Panahi. New J Chem **42**, 11137 (2018)
27. A. Singh, K. Vaishagya, R.K. Verma, R.Shukla. AAPS PharmSciTech **20**, 213 (2019)
28. Y.C. Chen, C.L. Lo, G.H. Hsiue, J Biomed Mater Res A. **102**, 2024 (2014)
29. T.Kavitha, I.K.Kang, S.Y.Park, Colloids Surf. B **115**, 37 (2014)
30. M.N. Mohammed, K. B.Yusoh, J.H.B.H. Shariffuddin, Mater. Res. Express **8**, 21 (2018)
31. K.M. Rao, B. Mallikarjuna, K.S.V.K. .Rao, S. Siraj, K. C.Rao, M. C. S. Subha. Colloids Surf. B **102**, 891 (2013)
32. M.Beija, J.D..Marty, M.Destarac. Chem.Comm **47**, 2826 (2011)
33. D.S. Chauhan, S. Indulekha, R. Gottipalli, B.P.K. Reddy, T.R. Chikate, R. .Gupta, D.N. Jahagirdar, R.Prasad, A. De, R.Srivastava. RSC Adv. 7, 44026 (2017)
34. M.N. Mohammed, K.B. .Yusoh, J.H.B.H.Shariffuddin. Mater. Res. Express **8**, 21 (2018)
35. S. Banihashem, Ma.N. Nezhati, H.A.Panahia. Carbohydr **227**, 115333 (2020)
36. T.Higuchi. J. Pharm. Sci. 52, 1145 (1963)
37. R.W. Korsmeyer, R. Gurny,, E.Doelker,,P.Buri,,N.A. Peppas, Int. J. Pharm. **15**, 25 (1983)
38. R. Salehi, M.Irani,M. Eskandani, K. Nowruzi, S. Davaran, I.Haririan. Int. **J**. Polym. Mater. **63**, 609 (2014)
39. B.F. Dizaji, M.H. Azerbaijan, N. Sheisi, P. Goleij, T. Mirmajidi, F. Chogan, M. Irani, F.Sharafian. Int. J. Biol. Macromol. **164**, 1461 (2002)
40. J. You, W. Li, C. Yu, C. Zhao, L. Jin, Y. Zhou, O. Wang, O. J. Nanoparticle Res. **15**, 1 (2013)
41. S. Guo, Y. Qiao, W. Wang, H. He, L. Deng, J. Xing, A. Dong, J. Mater. Chem. **20**, 6935 (2010)
42. Z. Liang, Z. Yang, H. Yuan, C. Wang, J. Qi, K. Liu, R. Cao, H.Zheng. Dalton Trans. **47**, 10223 (2018)
43. E.Y. Kim, H.S. Kim, D. Kim, J. Kim, P. S. Lee. *Crystals* **9**, 15 (2019)

Figures

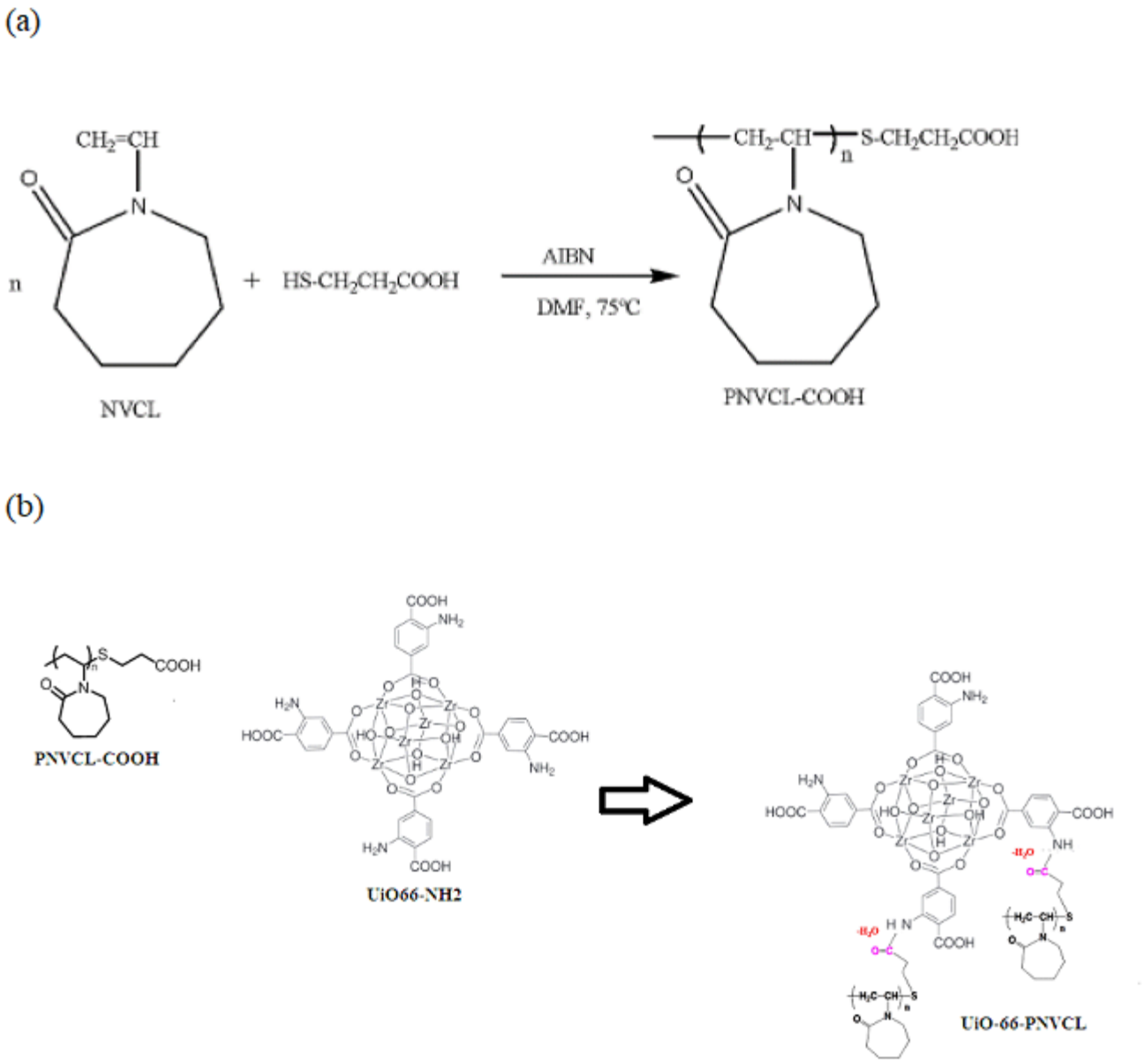

Figure 1

(a) Mechanism of the synthesis of (a) PNVCL and (b) UiO-66/NH2/PNVCL

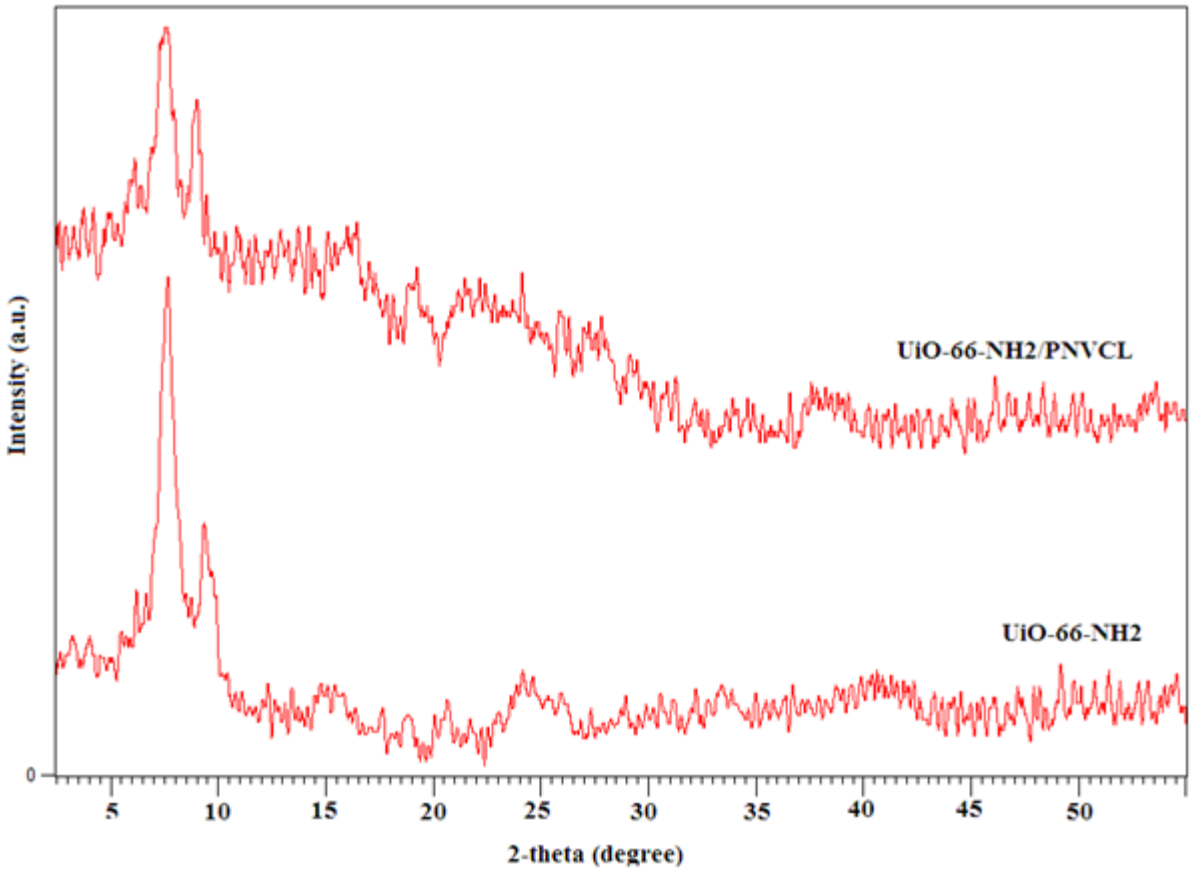

Figure 2

XRD patterns of UiO-66-NH2 MOF and PNVCL coated- UiO-66/DOX MOF nanoparticles

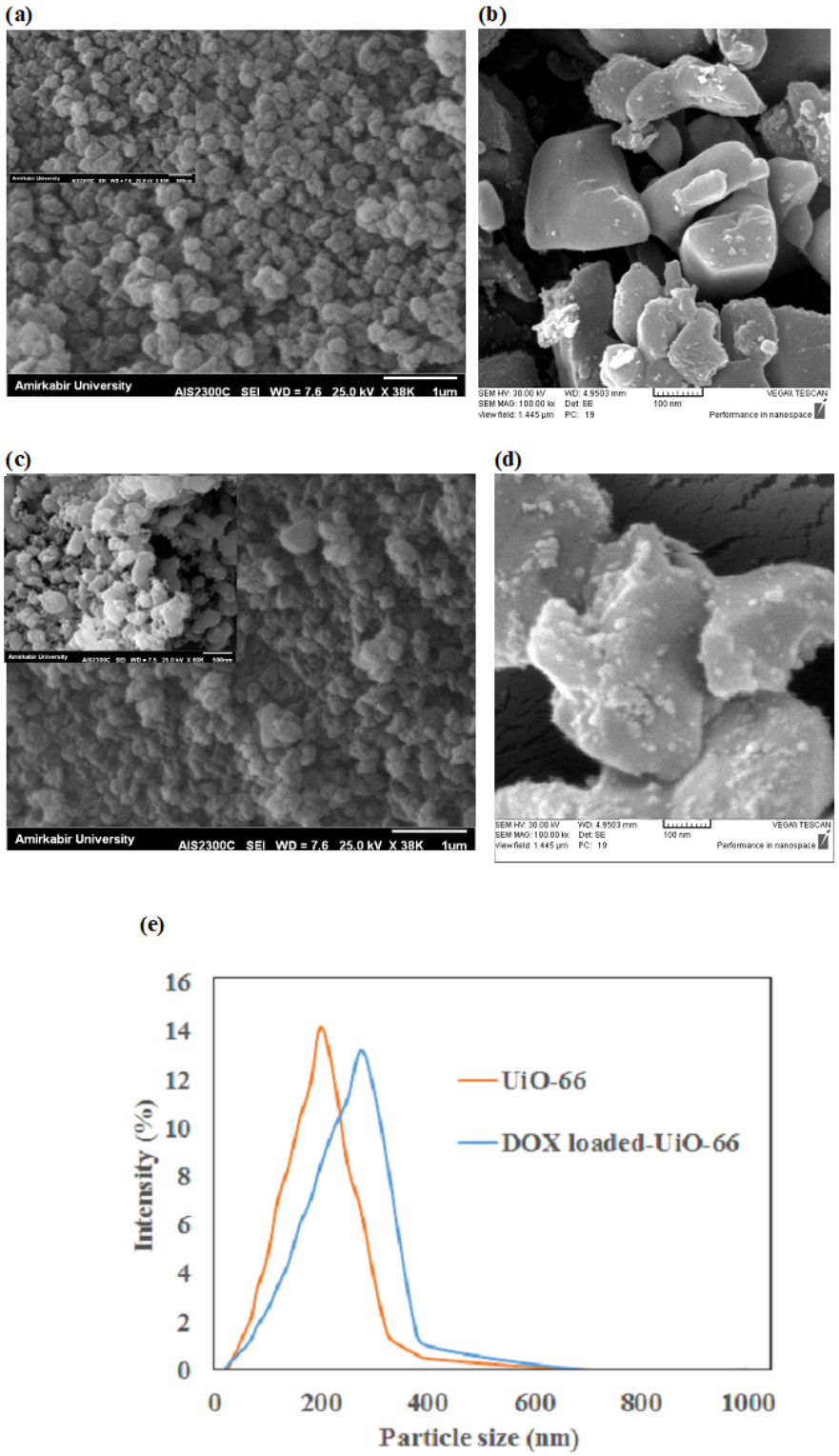

Figure 3

(a) SEM and (b) FESEM images of UiO-66-NH2 MOF (c) SEM and (d) FESEM images PNVCL 1% coated-UiO-66-NH2/DOX MOF nanoparticles and (e) DLS of UiO-66-NH2 NMOFs and DOX loaded-UiO-66-NH2 NMOFs

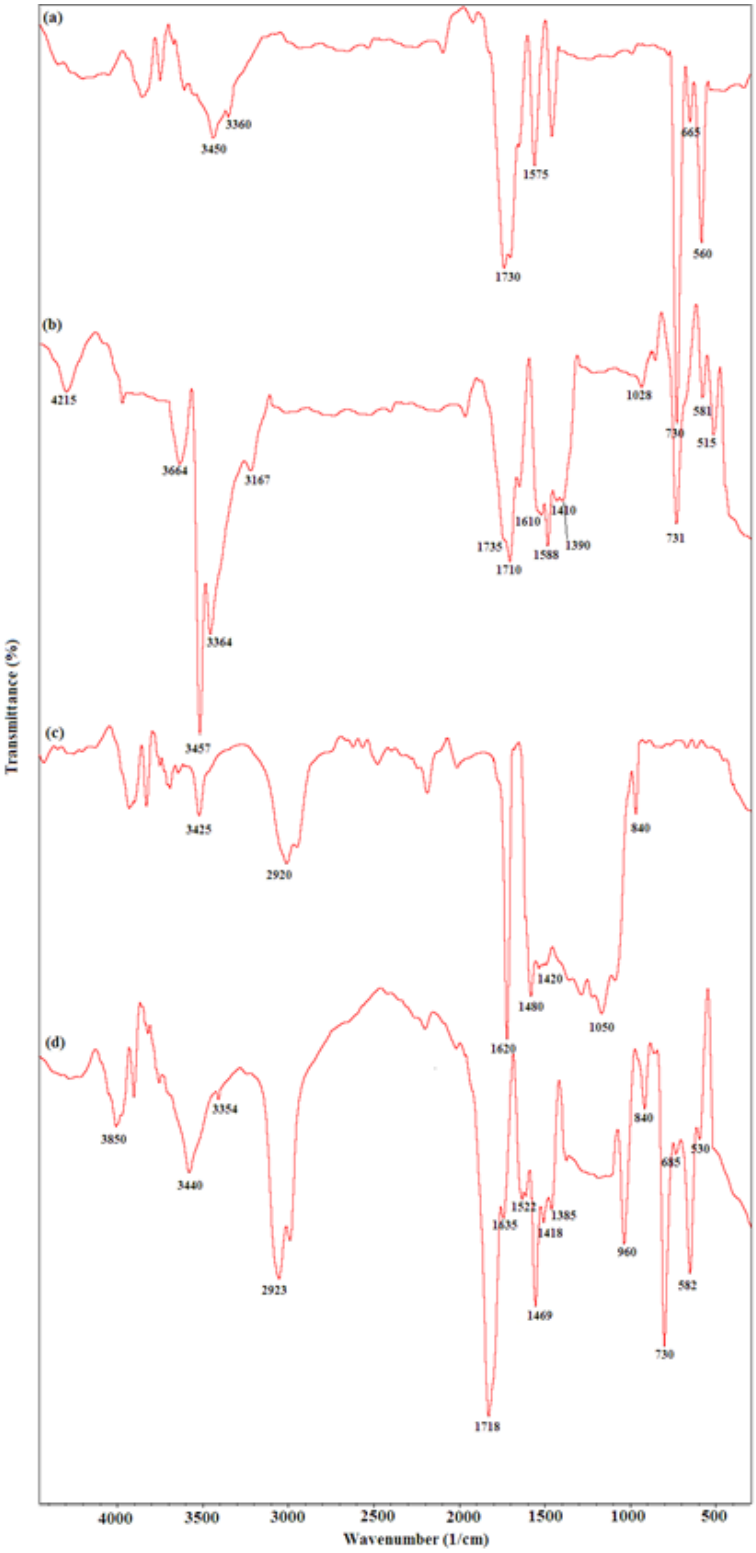

Figure 4

FTIR spectra of (a) UiO-66-NH2, (b) UiO-66-NH2/DOX, (c) PNVCL and (d) UiO-66/DOX/PNVCL

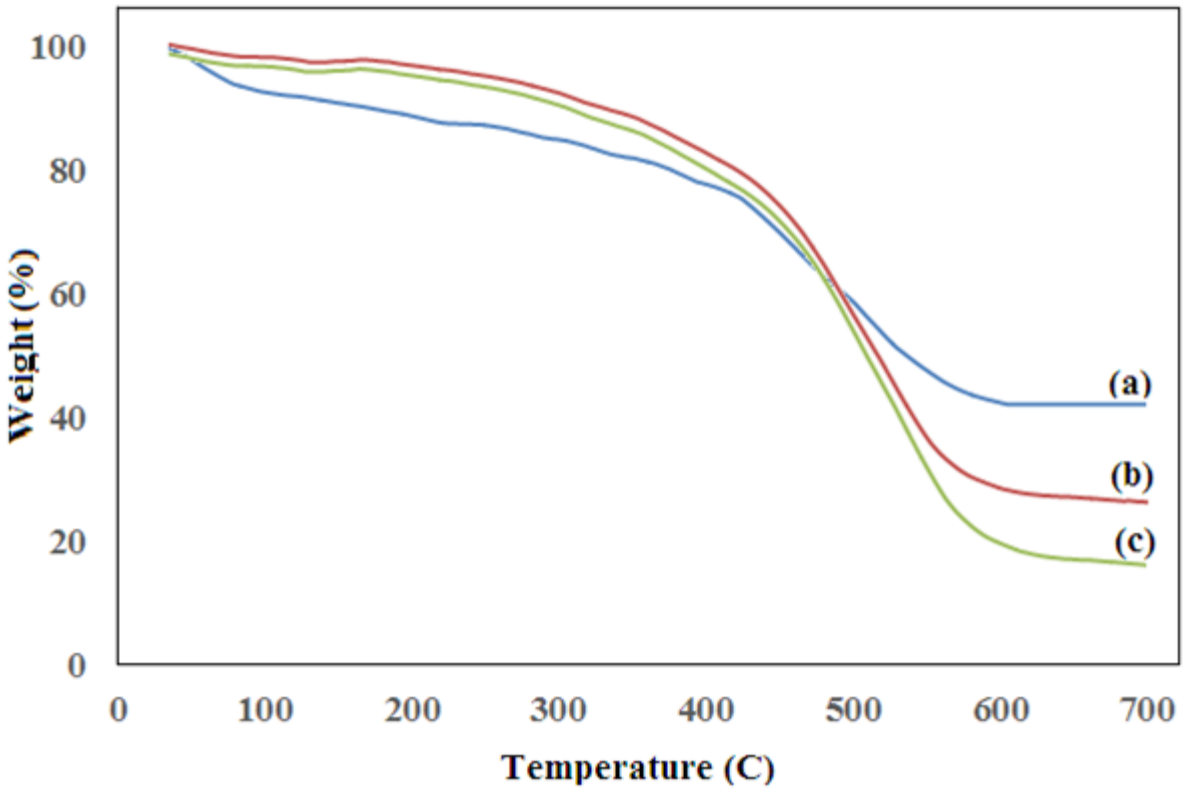

Figure 5

TGA curves of (a) UiO-66-NH2 NMOFs, (b) PNVCL 1%, (c) PNVCL 2% coated-UiO-66-NH2 NMOFs

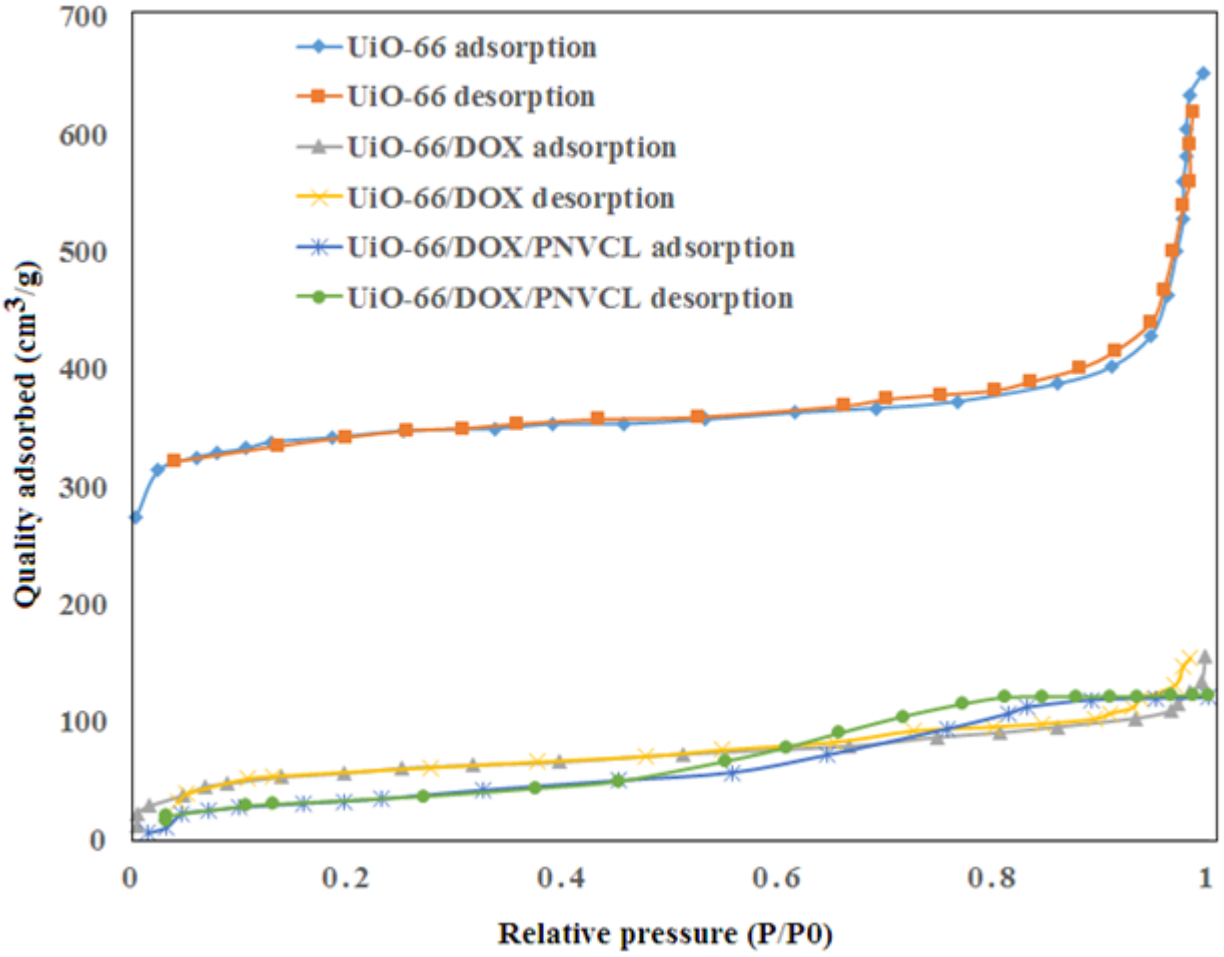

Figure 6

Nitrogen adsorption/desorption isotherms of UiO-66-NH2, UiO-66-NH2/DOX and UiO-66-NH2/DOX/PNVCL samples

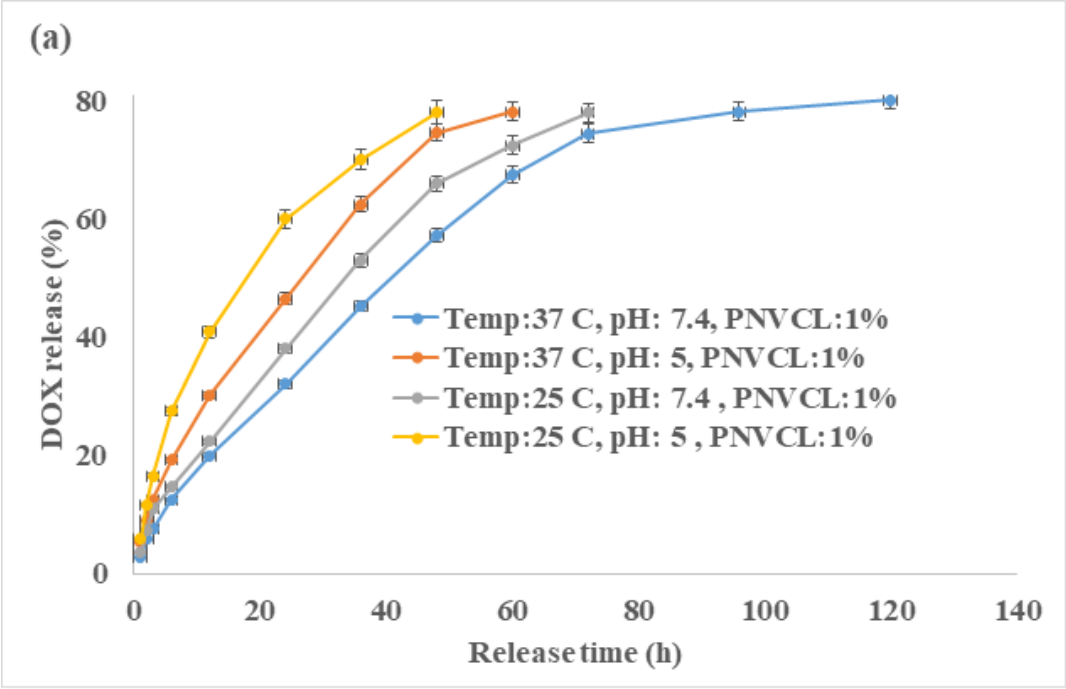

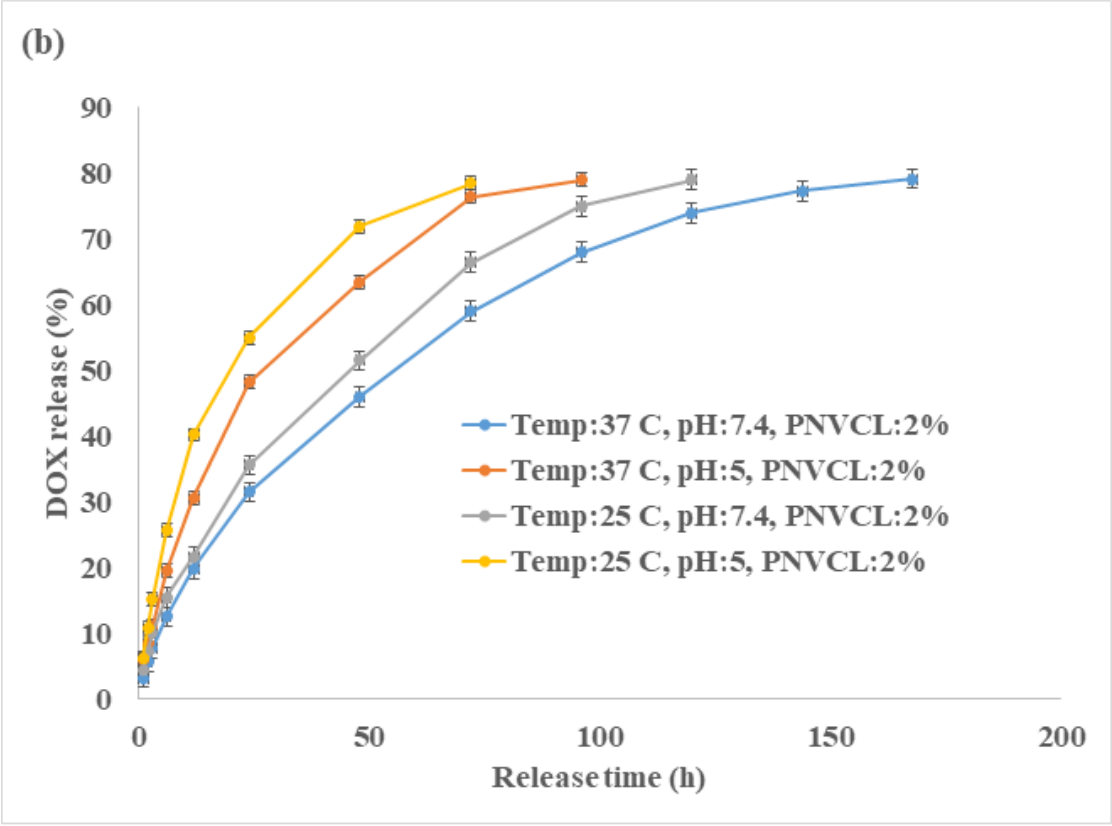

Figure 7

DOX release profiles of (a) PNVCL 1% coated- NMOFs and (b) PNVCL 2% coated- NMOFs containing 50 µg mL-1 DOX under temperatures of 25 °C, 37 °C and pH values of 5.5 and 7.4

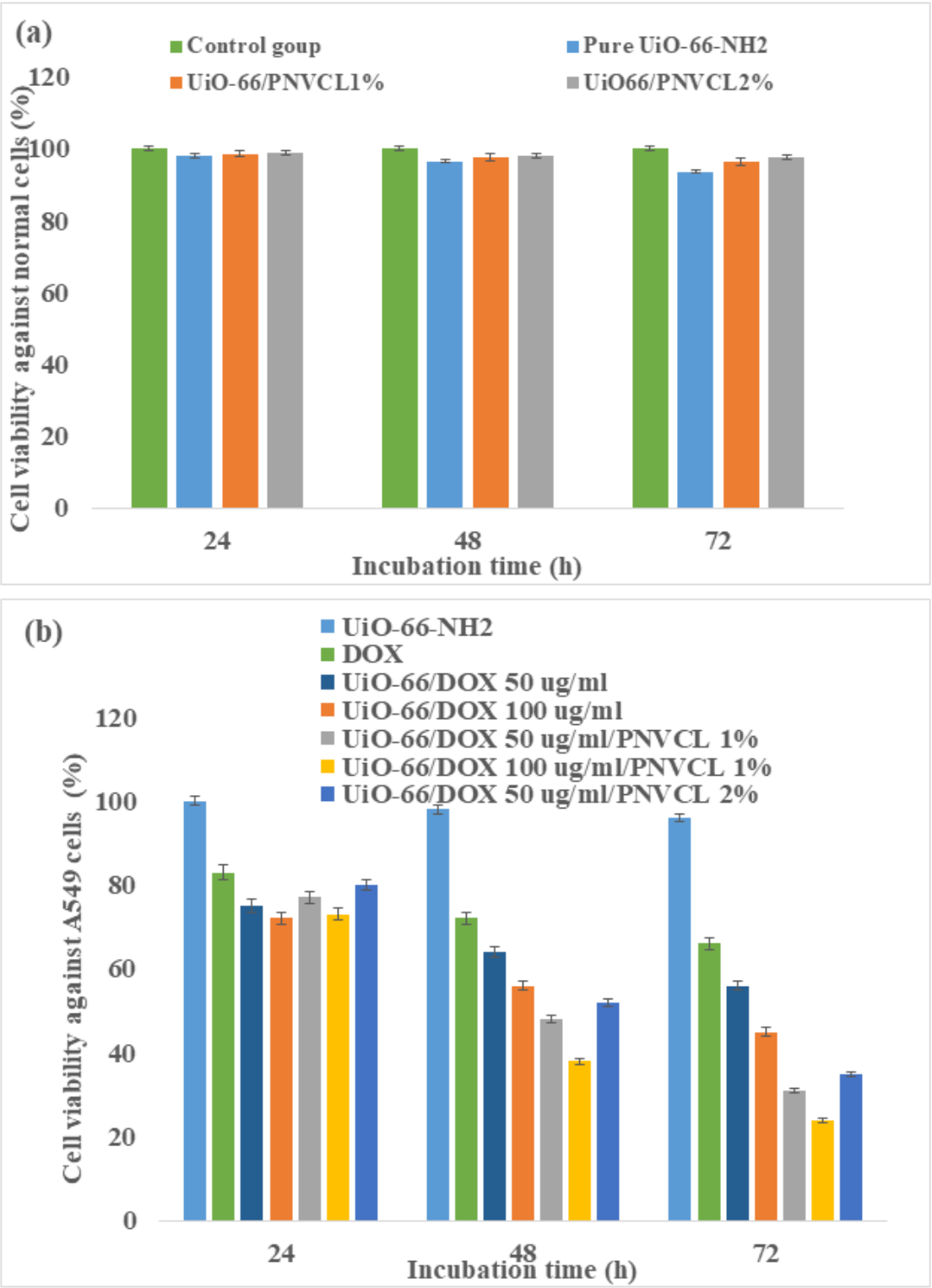

Figure 8

Cell viability of NMOFs samples against (a) normal fibroblast cells and (b) A549 lung cancer cells

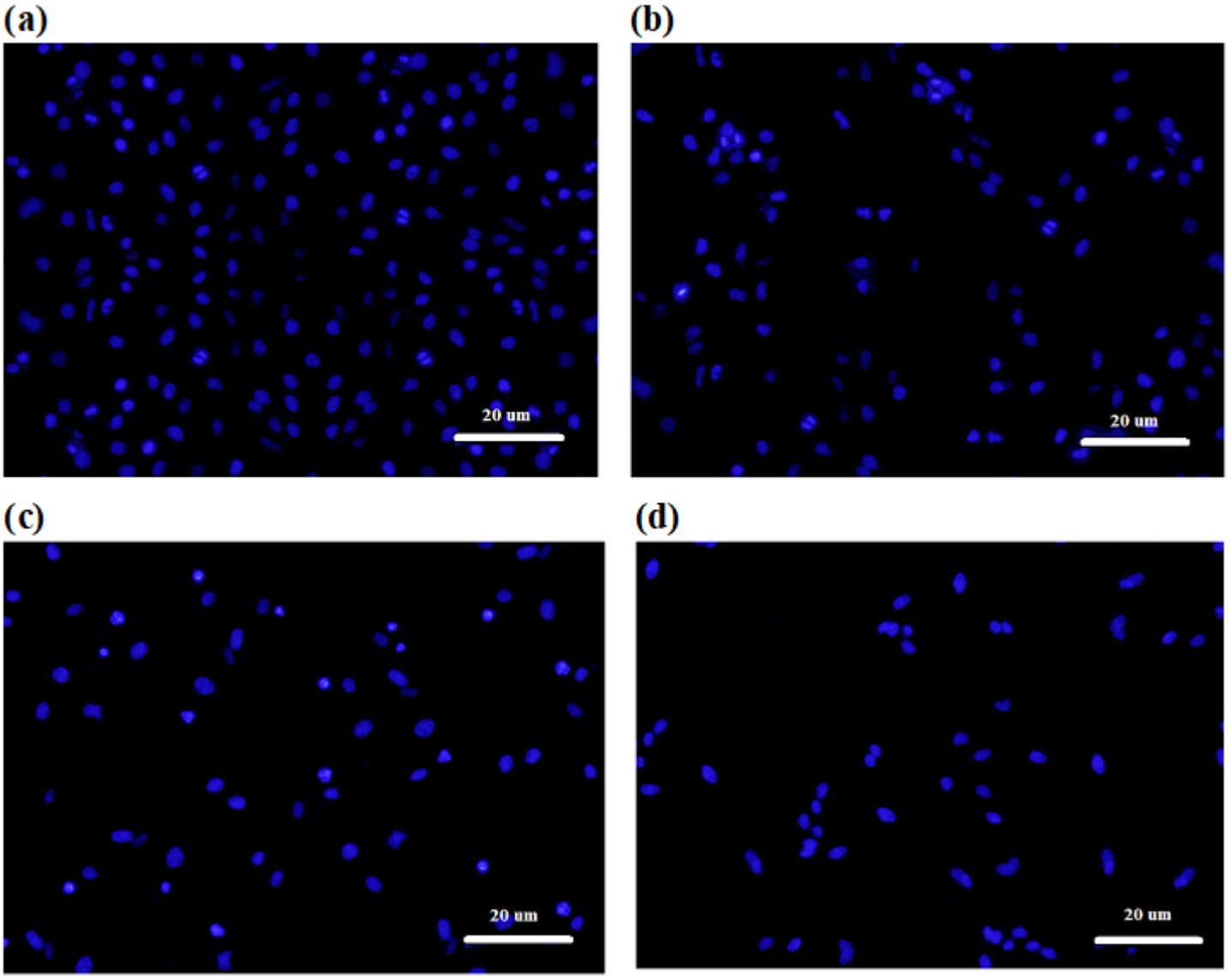

Figure 9

DAPI staining of (a) A549 cells and A549 cells treated (b) UiO-66-NH2/DOX 100 µg mL-1 NMOFs and NMOFs coated with (c) 1% and (d) 2% PNVCL after 72 h incubation time